

Robust Transient Stability Assessment via Reachability Analysis

Dongchan Lee

Department of Mechanical Engineering
Massachusetts Institute of Technology
Cambridge, MA
dclee@mit.edu

Konstantin Turitsyn

Department of Mechanical Engineering
Massachusetts Institute of Technology
Cambridge, MA
turitsyn@mit.edu

Abstract—Power system transient stability assessment studies the ability of the system to maintain synchronism under disturbances. The continuous effort on integrating renewable energy sources to the grid has created the need for stability assessment techniques that reflect the growing uncertainties. Reachability analysis has been recently proposed to address the issue with the uncertain initial operating condition by solving the relaxed linear optimization problem. Unlike conventional single-point simulation, reachability analysis performs a time domain simulation of a set described by a polytope. The polytope trajectory contains all possible simulation trajectories, and the convergence of the polytope towards the equilibrium is a sufficient condition for robust stability against the bounded uncertain initial condition. In this paper, we present the result on a second order swing equation model to explore the convergence condition of reachability analysis. We examine the relaxation gap introduced by the relaxation and relate the convergence to the contraction analysis.

I. INTRODUCTION

Transient stability ensures that generators remain synchronized after large disturbances, such as fault and generation re-dispatch [1], [2]. Due to the nonlinear dynamics and the scale of power systems, the transient stability still remain a challenging task. Moreover, the power system operates in a constantly changing environment where such variables are generation, loads, topology and operating parameters [1]. The recent integration of renewables adds more uncertainty in the operating environment, and we need new approaches to reliably address these issues.

The dominant approach in practice for transient stability assessment is the time-domain simulation, which relies on the known initial condition and system parameters [3]. The introduction of uncertainty requires sampling-based approaches, which requires a large amount of simulations [4]. From the simulated points, the security assessment has to be inferred to compute the secure region [5], [6]. The second most popular approach is the direct energy method, which uses the Lyapunov function to certify the stability [7], [8]. The conventional methods find the unstable equilibrium point on the conventional energy function. More recent approaches use semidefinite programming to find the stable region [9], [10]. However, the order of the generator model has to be kept low in order to have a tractable Lyapunov function. In addition, the energy function approach loses information

about the trajectories of the solution. There is a possibility of violating security constraints along the trajectories [11], [12], and computing the bounds on the trajectory with energy function methods is difficult.

To take account of uncertainties in transient stability assessment, we propose an idea of set simulation, where a set of operating points are simulated rather than a single point. A related work is the interval analysis, which has been introduced to take account of numerical errors with interval bounds [13], [14]. This type of bounding on the trajectories were explored in the power systems application [15], however, these methods were not applicable for concluding stability due to the lack of contraction of the set. Alternatively, an optimization-based reachability analysis using a polytope was proposed in [16], [17] for polynomial systems. However, the approach introduced in those papers is limited to a polynomial systems, and the algorithms are not scalable with respect to the state dimension of the system. In [18], the polytopic template along the modes of the system was proposed to make the analysis scalable for power systems application. Forming the polytope around the modes of the system allows the number of hyperplanes to be linear with respect to the system size. The nonlinear dynamics are tackled with the direct outer-approximation to relax the problem into linear programming, which is most tractable optimization problem [19], [20].

While the convergence of the polytope towards the equilibrium can guarantee the stability of a set, the gap between the actual trajectories and the reachability analysis grows in time due to the relaxation gap and imposing a fixed shape of the polytope as a constraint. The contraction of the polytope is necessary for the convergence of the trajectories, and we show the relation of the reachability analysis to the contraction analysis [21]. Contraction analysis is also useful for finding the region of attractions in transient stability [22]. In this paper, we will look at the convergence condition by looking at the contraction rate of the polytope. The polytope will contract as long as the contraction rate is larger than the relaxation gap. We show that the relaxation gap is very small when the input bound for the outer-approximation is small. Since the input bound is essentially the diameter of the polytope in the input variables, the polytope will contract in the presence of the relaxation gap as long as the input bound is small enough.

While the reachability analysis can be applied to higher order generator shown in [18], we present our study on a second order swing equation to analytically state the relaxation gap. We show the contraction of the polytope in 2 bus system and 39 bus system.

II. PROBLEM FORMULATION

A transmission line or generator contingency on power systems is a common cause of loss of synchronism. The existence of the feasible solution is insufficient, and the dynamic stability of the system should be studied as well in order to ensure the security of the grid. In this paper, we consider the second order swing equation with Kron reduction, which is widely used:

$$m_k \ddot{\delta}_k + d_k \dot{\delta}_k + \sum_{j \in \mathcal{N}_k} a_{kj} \sin(\delta_k - \delta_j) = P_{mk} \quad (1)$$

where m_k , d_k and P_{mk} are the inertia, damping and mechanical power injection at bus k , respectively. $a_{kj} = B_{kj} V_k V_j$ is the constant as we assume that the voltage is strictly regulated to 1 p.u. We note that our proposed method can be applied to a generalized high order swing equation, which was shown in [18]. We can rewrite the swing equation with the following compact vector notation,

$$\begin{aligned} \dot{\delta} &= \omega \\ \dot{\omega} &= M^{-1}(-D\omega - E^T X^{-1} \sin(E\delta) + P_{inj}). \end{aligned} \quad (2)$$

where M , D and X are diagonal matrix with diagonal entries being the inertia and damping of generators and line impedance respectively. P_{inj} is a vector of power injection. This is in a standard form for an ordinary differential equation, $\dot{x} = f(x)$, where the state of the system is $x = [\delta^T \omega^T]^T$. Our formulation will consider Explicit Euler method with time step Δt ,

$$x^{(t+1)} = x^{(t)} + \Delta t f(x^{(t)}). \quad (3)$$

The time stepping technique changes continuous ordinary differential equations into a set of discrete algebraic equations, and we will exploit this method to develop our algorithm. These algebraic equations will become a constraint for the optimization problem, and the Explicit Euler method allows effective bounding of nonlinearity in dynamic equation, $f(x)$. While the conventional simulation based approach solves the trajectories of an ordinary equation of a single point, we propose an algorithm that can simulate a neighborhood of states defined by a closed polytope denoted by

$$Ax^{(t)} \leq b^{(t)}, \quad (4)$$

where $A \in \mathbb{R}^{n \times m}$ and m is the number of hyperplanes in the polytope. Given the polytope template A , we solve the shifts of the hyperplane, $b^{(t)}$ at every time step. We take advantage of the polytope that each hyperplane is linear and can be computed separately. This yields the computation to be decomposed into simpler problems with linear objectives.

Given the current states confined in a polytope, the polytope at the next time step will contain every possible state that the current state is projected in time with a fixed time step.

We want to find $Ax^{(t+1)} \leq b^{(t+1)}$ so that it contains every possible $x^{(t+1)}$ originating from $Ax^{(t)} \leq b^{(t)}$. Finding such $b^{(t+1)}$ involves an optimization problem as we want to find maximum $b^{(t+1)}$ that is reachable from $Ax^{(t)} \leq b^{(t)}$. The optimization problem is generally a non-convex problem for a nonlinear system. Solving the relaxed problem is sufficient to certify the containment of all reachable space. The polytope formed by solving a relaxed problem will contain the polytope formed by solving the original problem, and thus will contain all reachable space. In general, the number of faces of the polytope can grow enormously with respect to the system size, but the construction of the polytope around the mode can restrict the number of faces to grow linearly with respect to the system size.

A. Template Construction

In this section, we show how the template, $A \in \mathbb{R}^{m \times n}$ is constructed around the equilibrium. Consider the linearized system dynamic at the equilibrium to be $\dot{x} = Jx$ with the eigenvalue decomposition in the real system representation, $J = Q\Lambda Q^{-1}$. We denote each block of Λ as $\Lambda_{(l)}$ so that $\Lambda = \text{blkdiag}(\Lambda_{(1)}, \dots, \Lambda_{(L)})$ where the real system representation gives $\Lambda_{(l)} = \lambda_l$ for real eigenvalue and $\Lambda_{(l)} = \begin{bmatrix} \sigma_l & \omega_l \\ -\omega_l & \sigma_l \end{bmatrix}$ for complex conjugate pair. We construct a matrix $A = \hat{A}Q^{-1}$ such that $\hat{A} = \text{blkdiag}(\hat{A}_{(1)}, \dots, \hat{A}_{(L)})$ and $\hat{A}_{(l)}$. The construction rule is as follows:

- 1) If the eigenvalue at block (l) is real, then $\hat{A}_{(l)} = \begin{bmatrix} 1 & -1 \end{bmatrix}^T$
- 2) If the eigenvalues at block (l) are a complex conjugate pair, then

$$\hat{A}_{(l)} = \begin{bmatrix} \cos(\psi_1) & \sin(\psi_1) \\ \vdots & \vdots \\ \cos(\psi_{m_l}) & \sin(\psi_{m_l}) \end{bmatrix}$$

where $\psi_k = \frac{2k\pi}{m_l}$ and m_l are chosen to be an even number that satisfy the inequality, $\tan\left(\frac{\pi}{m_l}\right) < \left|\frac{\sigma_l}{\omega_l}\right|$.

This construction method of the polytope considers the dynamic at the equilibrium and builds naturally around the mode. This polytope is guaranteed to converge if the linearized system at the equilibrium is stable. The number of hyperplanes is even so that each hyperplane has its pair facing the opposite direction. We will define Δx as the distance between these pairs in the later section and may refer to it as the diameter of the polytope.

B. Dynamic Template

After constructing the initial template, the template is updated at every time step to capture the change in the template due to the dynamics. The dynamic template approach was introduced in [16], and the update rule is given as follows:

$$A^{(t+1)} = A^{(t)} \cdot (I + \Delta t \cdot J(\tilde{x}^{(t)}))^{-1} \quad (5)$$

where $\tilde{x}^{(t)}$ is an approximate mid-point of the polytope. This point can be computed by direct simulation of the mid-point

in the initial polytope or by computing the centroid of the polytope at every time step. The dynamic template may not align with the modes of the system after going through the nonlinear dynamics, so the dynamic can be truncated with the original template that is fixed. After updating the polytope template, the only computation left is $b^{(t+1)}$ in order to fully describe the set. Computing the polytope at every step can be formulated as an optimization problem of solving $b^{(t+1)}$ that bounds all possible states, $x^{(t+1)}$. This problem can be written as

$$\begin{aligned} & \underset{x^{(t)}, x^{(t+1)}}{\text{maximize}} && A_i^{(t+1)} \cdot x^{(t+1)} \\ & \text{subject to} && x^{(t+1)} = x^{(t)} + \Delta t \cdot f(x^{(t)}) \\ & && A^{(t)} x^{(t)} \leq b^{(t)} \end{aligned} \quad (6)$$

where we try to maximize the location of the hyperplane, A_i , at the next time step. The dynamic and the bounds on the current state constrain the possible state in the next time step. This problem has to be solved for every hyperplane in the polytope. Due to the non-linearity of power systems, this is a non-convex problem and is hard to solve in general.

III. RELAXED LINEAR OPTIMIZATION

We propose the relaxation of this problem based on the outer-approximation of nonlinearity in the constraint. In the case for the second order swing equation, the source of nonlinearity is from the sine function. We confine the nonlinearity into a separate variable and develop a precomputed outer-approximation.

$$\begin{aligned} & \underset{x^{(t)}, x^{(t+1)}}{\text{maximize}} && A_i^{(t+1)} \cdot x^{(t+1)} \\ & \text{subject to} && \delta^{(t+1)} = \delta^{(t)} + \Delta t \cdot \omega^{(t)} \\ & && \omega^{(t+1)} = \omega^{(t)} + \Delta t \cdot M^{-1}(-D\omega^{(t)} \\ & && \quad - E^T X^{-1}u + P_{inj}) \\ & && A^{(t)} x^{(t)} \leq b^{(t)} \\ & && u \in \langle \sin(E\delta^{(t)}) \rangle \end{aligned} \quad (7)$$

where $\langle \sin(E\delta^{(t)}) \rangle$ is the sine envelope, and $x = [\delta^T \omega^T]^T$. The outer-approximation is especially powerful in our formulation because the dynamics of interest are confined by the polytope. Within this polytope, the dynamic can be approximated very well via linearization. Then, a polytope can approximate the function tightly and minimize the gap between the original and relaxed problems.

A. Sine Envelopes

The outer-approximation of the sinusoidal function replaces the nonlinear function by linear inequalities. Our envelope further exploit the bound on the generator angles $\delta^{(t)}$ to develop very tight linear bounds. Since the gap from solving this type of optimization accumulate over time, it is important to minimize the gap between the original and relaxed problem. Given the function $u = \sin(\delta)$ with $\underline{\delta} \leq \delta \leq \bar{\delta}$, $|\underline{\delta}| \leq \pi$ and $|\bar{\delta}| \leq \pi$, the linear envelope can be categorized to three cases.

This is a sine envelope without phase shift developed in [18], and it extends the range to be between $-\pi$ to π . Figure 1 illustrates examples of the categorized cases.

1) *Convex/Concave Region*: For $0 \leq \underline{\delta} \leq \bar{\delta}$ and $\underline{\delta} \leq \bar{\delta} \leq 0$, the function is concave and convex respectively. In this case, the first order condition at the boundary points, the chord between boundary points, and the boundary from the mean value theorem can be used for the linear envelope. Let $m_{a,b}$ be the slope of the chord between point a and b , $m_{a,b} = \left(\frac{\sin(a) - \sin(b)}{a - b}\right)$. In the convex case, the linear envelope is as follows:

$$\begin{aligned} u &\geq \cos \bar{\delta}(\delta - \bar{\delta}) + \sin \bar{\delta} \\ u &\geq \cos \underline{\delta}(\delta - \underline{\delta}) + \sin \underline{\delta} \\ u &\leq m_{\bar{\delta}, \underline{\delta}}(\delta - \bar{\delta}) + \sin \bar{\delta} \\ u &\geq m_{\bar{\delta}, \underline{\delta}}(\delta - \cos^{-1} m_{\bar{\delta}, \underline{\delta}}) + \sin(\cos^{-1} m_{\bar{\delta}, \underline{\delta}}) \end{aligned} \quad (8)$$

For the concave case, inequality signs can be changed to the other side.

2) *Chord-connected Region*: If the region is not convex or concave but the function in the given input bound either lies above or below the chord, we classify this case as a chord-connected region. In this case, we define the following points: $\varphi_{\bar{\delta}} = \max\{\varphi \mid \cos \varphi = \left(\frac{\sin(\bar{\delta}) - \sin(\delta)}{\varphi - \bar{\delta}}\right), \varphi < \bar{\delta}\}$ and $\varphi_{\underline{\delta}} = \min\{\varphi \mid \cos \varphi = \left(\frac{\sin(\underline{\delta}) - \sin(\delta)}{\varphi - \underline{\delta}}\right), \varphi > \underline{\delta}\}$. The point, φ_{δ} is the that its derivative tangent to the chord between δ and φ_{δ} . Since this is a point that has to satisfy the equality of a nonlinear function, the Newton-Raphson algorithm should be used to identify this point. This can be computed very quickly since the function and variable are scalar. If the function lies below the chord, then the following constraints describe the outer-approximation:

$$\begin{aligned} u &\geq m_{\varphi_{\bar{\delta}}, \bar{\delta}}(\delta - \bar{\delta}) + \sin \bar{\delta} \\ u &\geq \cos \underline{\delta}(\delta - \underline{\delta}) + \sin \underline{\delta} \\ u &\leq \Delta m_{\bar{\delta}, \underline{\delta}}(\delta - \bar{\delta}) + \sin \bar{\delta} \\ u &\geq \Delta m_{\bar{\delta}, \underline{\delta}}(\delta - \cos^{-1} m_{\bar{\delta}, \underline{\delta}}) + \sin(\cos^{-1} m_{\bar{\delta}, \underline{\delta}}). \end{aligned} \quad (9)$$

If the function lies above the chord, the above constraints with the inequality signs changed to the other side can be used.

3) *Chord-crossing Region*: For the case that the function crosses the chord at any point within the input bound, the chord constraint cannot be used. In this case, we can use the following constraints:

$$\begin{aligned} u &\geq \cos \bar{\delta}(\delta - \bar{\delta}) + \sin \bar{\delta} \\ u &\geq \cos \underline{\delta}(\delta - \underline{\delta}) + \sin \underline{\delta} \\ u &\geq m_{\bar{\delta}, \varphi_{\bar{\delta}}}(\delta - \bar{\delta}) + \sin \bar{\delta} \\ u &\geq m_{\varphi_{\underline{\delta}}, \underline{\delta}}(\delta - \underline{\delta}) + \sin \underline{\delta}. \end{aligned} \quad (10)$$

The input bound shown in Figure 1 (c) and (d) belongs to this case.

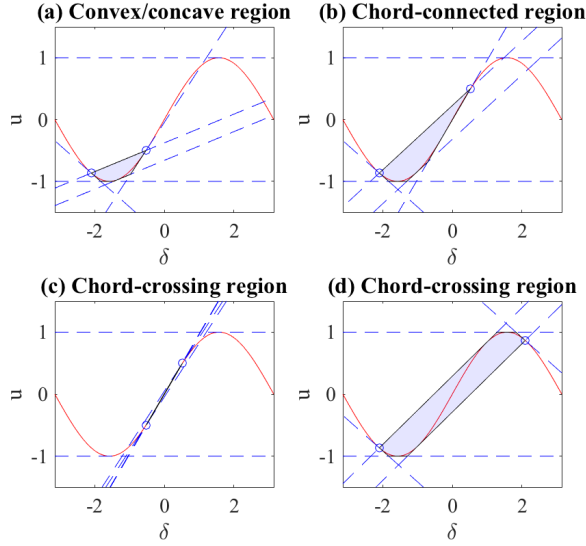


Fig. 1. The outer-approximation for the sine function is presented. The given bound is marked with blue circles, and the polytope approximation is colored with light blue.

IV. ANALYSIS ON THE CONVERGENCE OF REACHABILITY ANALYSIS

A. Gap from Outer-Approximation

In this section, we present the relaxation gap from using the outer-approximation of the sine function. The gap of the outer-approximation for a sinusoidal function can be explicitly written, and we can bound the relaxation gap in the optimization problem in Equation 7. Given the upper and lower input bound, we can explicitly compute the maximum possible gap. This gap is drawn in Figure 2.

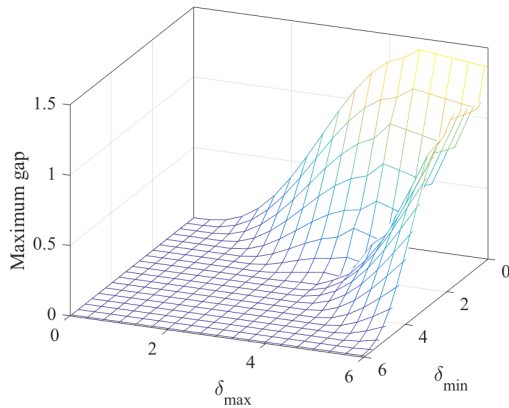


Fig. 2. The outer-approximation gap for the sine function.

The relaxation gap increases with the size of the input bound as we expected. The bound is lower near $\delta = 0$ since this region can be approximated by a linear function very well. In this case, the gap is very small as shown in Figure 1 (c). To simplify our analysis, we can focus on the size of the input

bound without specifying its location. We denote the size of the input bound as $\Delta\delta = \bar{\delta} - \underline{\delta}$, and Figure 3 shows the same picture as Figure 2 projected to $\Delta\delta$.

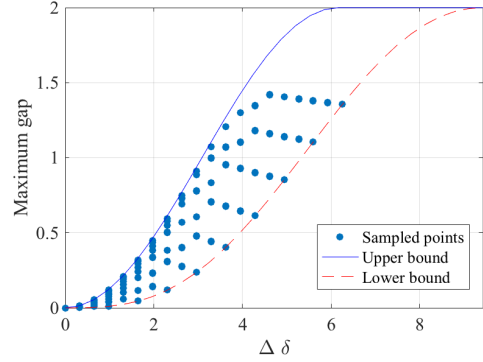


Fig. 3. The outer-approximation gap for the sine function with respect to the size of the input bound. The upper and lower bound on this gap is shown as a function of input bound size.

In this case, we can explicitly state the bound on the gap between the outer-approximation and the original function. Given the bound $\Delta\delta \leq 2\pi$, the gap between the original sine function and outer-approximation will be

$$|\sin(\delta) - \langle \sin(\delta) \rangle| \leq 2 \sin\left(\frac{\Delta\delta}{4}\right)^2. \quad (11)$$

where $\Delta\delta$ is the size of the input bound. This occurs when the input bound of size $\Delta\delta$ has its midpoint at $\frac{\pi}{2}$ or $-\frac{\pi}{2}$. For $\Delta\delta > 2\pi$, the maximum gap will be 2 since sinusoidal functions are bounded between -1 to 1. Although it may not be as useful as the upper bound, it is also possible to get an expression for the lower bound of maximum gap as follows:

$$|\sin(\delta) - \langle \sin(\delta) \rangle| \geq \Delta\delta \cos(\theta) - 2 \sin\left(\frac{\Delta\delta}{2}\right) \quad (12)$$

where $\theta = \min\{\theta \mid \cos\theta = \frac{\sin(\theta) + \sin(\Delta\delta/2)}{\theta + \Delta\delta/2}, \theta > 0\}$. This lower bound occurs when the input bound of size $\Delta\delta$ has its midpoint at 0. These two bounds are drawn in Figure 3 as well as sampled points. From the upper-bound of the maximum gap, the upper-bound on the relaxation gap in Equation 7 can be bounded as follows:

$$\epsilon = b - b^* \leq \left| 2\Delta t A \begin{bmatrix} 0 \\ M^{-1} E^T X^{-1} \sin\left(\frac{\Delta\delta}{4}\right)^2 \end{bmatrix} \right|. \quad (13)$$

The upper bound for the relaxation gap is a non-decreasing function with respect to the size of the polytope. In addition, the size of the system or lacking inertia increases the relaxation gap as well.

B. Convergence condition for a linear system with constant gap

In this section, we examine the condition for the convergence of the network in a linear system, $\dot{x} = Jx$ with a

fixed polytope template A . To simplify our statements, we will consider the initial polytope in the form of $A(x - \tilde{x}) \leq \mathbb{1}^m \cdot \tilde{b}^{(0)}$ where $\mathbb{1}^m$ is a vector of 1, $\tilde{b}^{(t)}$ is a scalar, and \tilde{x} is the relocated position of the polytope. In the standard form, $Ax \leq b = A\tilde{x} + \mathbb{1}^m \cdot \tilde{b}^{(0)}$. From the contraction analysis, we have a matrix measure of a polytopic norm, $\|x\|_A = \max Ax$, defined as

$$\mu_A(J) = \lim_{\varepsilon \rightarrow 0^+} \frac{\|I + \varepsilon J\| - 1}{\varepsilon} \quad (14)$$

where the matrix norm is defined as $\|J\| = \max_{x \neq 0} \frac{\|Jx\|_A}{\|x\|_A}$. This matrix measure can be numerically computed by solving

$$\begin{aligned} \mu_A(J) = \max_{x, i \in \mathbb{R}} \quad & A_i J x \\ \text{subject to} \quad & Ax \leq 1, \quad A_i x = 1. \end{aligned} \quad (15)$$

The matrix measure of our polytopic norm is the contraction rate of the current polytope, and the relaxation has to be less than the contraction rate for the polytope to converge to the equilibrium. Given the relaxation gap ϵ , the convergence condition is

$$\mu_A(J) + \frac{\epsilon}{\Delta t \tilde{b}^{(t)}} \leq 0. \quad (16)$$

where μ_A is the matrix measure at time t . To see this, we have

$$\begin{aligned} b_i^{(t+1)} - b_i^{(t)} = \max_{x^{(t)}, x^{(t+1)}} \quad & A_i \cdot x^{(t+1)} - b_i^{(t)} \\ \text{subject to} \quad & x^{(t+1)} = x^{(t)} + \Delta t J x^{(t)} \\ & A(x - \tilde{x}) \leq \mathbb{1}^m \cdot \tilde{b}^{(t)}. \end{aligned} \quad (17)$$

With direct substitutions of constraints into the objective, we get

$$b_i^{(t+1)} - b_i^{(t)} \geq \Delta t \tilde{b}^{(t)} \mu_A(J). \quad (18)$$

Since the condition on the relaxation gap for the contraction is $\epsilon \leq b_i^{(t)} - b_i^{(t+1)}$, we arrive in Equation 16. The inequality in Equation 16 can be interpreted as the contraction rate being greater than the relaxation gap. When the polytope contracts, it results in a tighter input bound for the next time step. Since the relaxation gap decreases rapidly with respect to the input bound as shown in Figure 3, the polytope contracts faster at every iteration once the size of the polytope is less than some threshold. Moreover, the reachability analysis with dynamic template in a linear system results in the exact set of trajectories. This result gives high chance for the reachability analysis in a nonlinear system to give a useful result by tightly bounding the nonlinearities.

In Figure 4, we show the contraction of the polytope size depending the the relaxation gap. When the relaxation gap is equal to the contraction rate, then the size of the polytope stays constant because the deflation from contraction is compensated by the inflation from the relaxation gap. When the contraction is stronger than the relaxation gap, it shows exponential convergence. In addition, we note that using the dynamic template contracts much faster than fixed template.

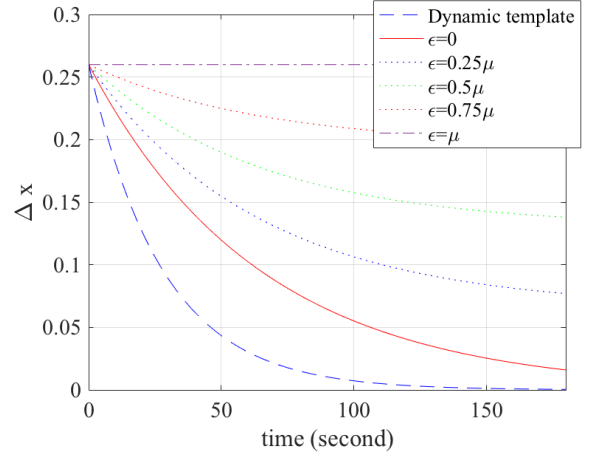


Fig. 4. Contraction of the polytope depending on the relaxation gap. We rescale $\mu = \Delta t b^{(0)} \mu_A(J)$ in this plot.

The fixed template has an accumulating error from imposing a certain shape, which result in a set that is larger than the exact set. The dynamic template accounts for this effect from the shape of the polytope and achieves faster convergence. The damping in the system decreases the matrix measure, so high damping result in stronger contraction and allow larger relaxation gap. An alternative view is considering the relaxation gap as uncertainties of the model. For a marginally stable system, uncertainties can play a critical role, making it much more difficult to converge.

V. CASE STUDIES

A. 2 bus system

In this section, we present result on a 2 bus system for illustration of our approach. Figure 5 shows the phase portrait of the system as well as the polytope computed at every time

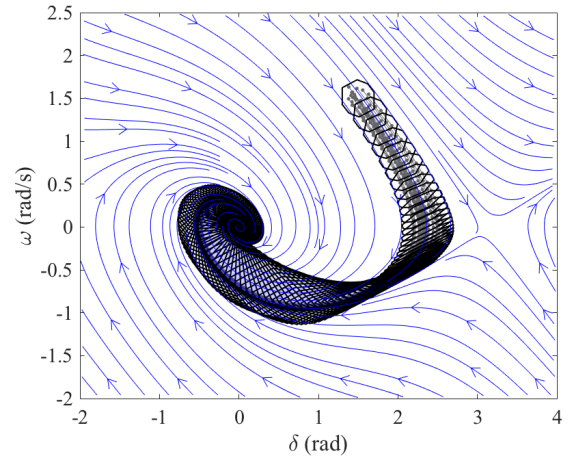


Fig. 5. The phase portrait of the dynamics as well as the polytopes computed with the reachability analysis is shown for a 2 bus system. In this case all the initial conditions converged to the equilibrium.

step. In this case, every trajectory from the initial operating point set is stabilized to the equilibrium. We note that this approach can survive near the unstable equilibrium point where the system becomes highly nonlinear in 2 dimensional analysis.

Figure 6 shows the Monte-Carlo simulation as well as the bound computed using the reachability approach. The bound is shown to be very tight to the Monte-Carlo simulation and converges to the equilibrium.

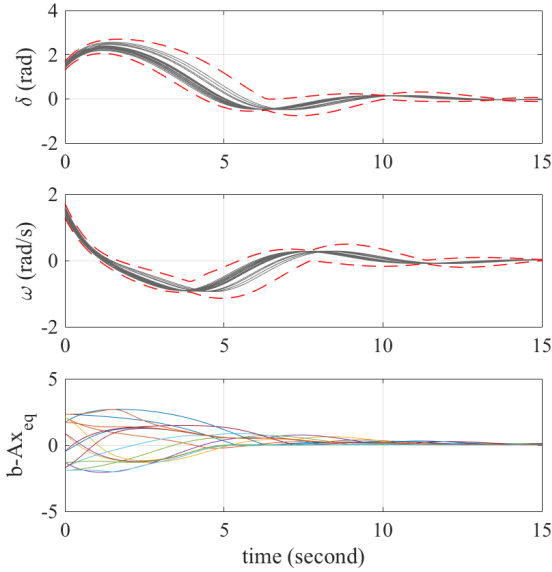


Fig. 6. The time domain simulation of the system based on the Monte-carlo simulation is shown. The red dashed lines are the bound from the reachability analysis. On the bottom, the distance of each planes from the equilibrium is shown, which converged to zero.

In Figure 7, the change in the size of the polytope is shown. The system experiences nonlinear transient effect until 7 seconds, and after that point, the polytope shows an exponential contraction.

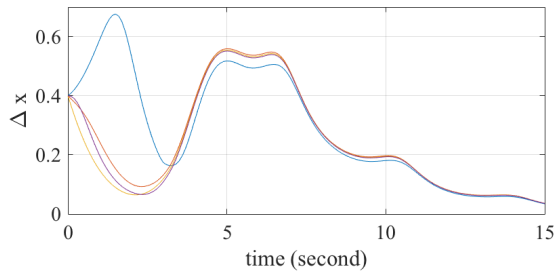


Fig. 7. Contraction of polytope size on a 2 bus system.

Figure 8 shows a case where the initial polytope goes through the unstable equilibrium. While some of the solutions are able to reach back to the equilibrium, the polytope grows due to the trajectories that do not converge to the desired equilibrium.

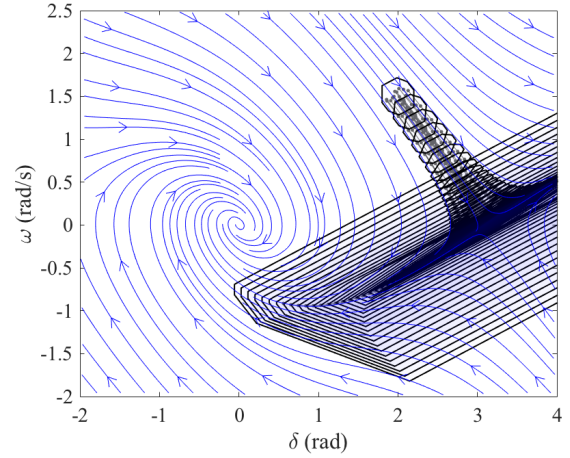


Fig. 8. Case study for an unstable case in 2 bus system is shown in this figure.

B. 39 bus system

In Figure 9, the contraction of the polytope is also shown. It also demonstrates an exponential convergence towards the equilibrium. According to Equation 13, the size of the network increases the relaxation gap, and it may need to be compensated by reducing the size of the polytope, which corresponds to reducing the bound on the uncertainties.

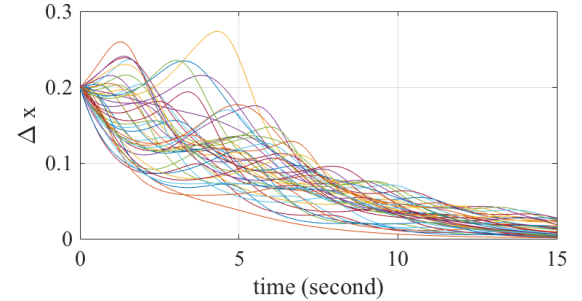


Fig. 9. Contraction of polytope size on a 39 bus system.

VI. CONCLUSION

In this paper, we present the reachability analysis approach for robust transient stability assessment. We explored the effect of the relaxation gap in solving the relaxed optimization problem in reachability analysis. We showed that the convergence condition is determined by the contraction rate and the relaxation gap. The contraction rate has to be greater than the relaxation gap in order for the polytope to converge and contract towards the equilibrium. The relaxation gap from the outer-approximation of the sinusoidal function is very tight with small input bound, and the use of dynamic template further reduces the accumulating errors. Currently, the dynamic template only considers the linear effect based on the approximate midpoint of the polytope, and the future work

includes exploring options for adding additional hyperplanes in the template that takes account for the nonlinear effect.

REFERENCES

- [1] P. Kundur, N. J. Balu, and M. G. Lauby, *Power system stability and control*. McGraw-hill New York, 1994, vol. 7.
- [2] J. Machowski, J. Bialek, and J. Bumby, *Power system dynamics: stability and control*. John Wiley & Sons, 2011.
- [3] M. Pavella, D. Ernst, and D. Ruiz-Vega, *Transient stability of power systems: a unified approach to assessment and control*. Springer Science & Business Media, 2012.
- [4] J. R. Hockenberry and B. C. Lesieutre, "Evaluation of uncertainty in dynamic simulations of power system models: The probabilistic collocation method," *IEEE Transactions on Power Systems*, vol. 19, no. 3, pp. 1483–1491, Aug 2004.
- [5] P. Kundur, G. K. Morison, and L. Wang, "Techniques for on-line transient stability assessment and control," in *2000 IEEE Power Engineering Society Winter Meeting. Conference Proceedings (Cat. No.00CH37077)*, vol. 1, 2000, pp. 46–51 vol.1.
- [6] D. Lee, P. Srikantha, and D. Kundur, "Secure operating region simplification in dynamic security assessment," in *2015 IEEE International Conference on Smart Grid Communications (SmartGridComm)*, Nov 2015, pp. 79–84.
- [7] H.-D. Chang, C.-C. Chu, and G. Cauley, "Direct stability analysis of electric power systems using energy functions: theory, applications, and perspective," *Proceedings of the IEEE*, vol. 83, no. 11, pp. 1497–1529, Nov 1995.
- [8] H.-D. Chiang, *Direct methods for stability analysis of electric power systems: theoretical foundation, BCU methodologies, and applications*. John Wiley & Sons, 2011.
- [9] T. L. Vu and K. Turitsyn, "Lyapunov functions family approach to transient stability assessment," *IEEE Transactions on Power Systems*, vol. 31, no. 2, pp. 1269–1277, March 2016.
- [10] —, "A framework for robust assessment of power grid stability and resiliency," *IEEE Transactions on Automatic Control*, vol. PP, no. 99, pp. 1–1, 2016.
- [11] F. Milano and R. Zárate-Miñano, "A systematic method to model power systems as stochastic differential algebraic equations," *IEEE Transactions on Power Systems*, vol. 28, no. 4, pp. 4537–4544, Nov 2013.
- [12] S. O. Faried, R. Billinton, and S. Aboreshaid, "Probabilistic evaluation of transient stability of a power system incorporating wind farms," *IET Renewable Power Generation*, vol. 4, no. 4, pp. 299–307, July 2010.
- [13] R. E. Moore, R. B. Kearfott, and M. J. Cloud, *Introduction to interval analysis*. SIAM, 2009.
- [14] L. Jaulin, "Nonlinear bounded-error state estimation of continuous-time systems," *Automatica*, vol. 38, no. 6, pp. 1079 – 1082, 2002.
- [15] H. N. V. Pico, D. C. Aliprantis, and E. C. Hoff, "Reachability analysis of power system frequency dynamics with new high-capacity hvac and hvdc transmission lines," in *2013 IREP Symposium Bulk Power System Dynamics and Control - IX Optimization, Security and Control of the Emerging Power Grid*, Aug 2013, pp. 1–9.
- [16] M. A. Ben Sassi, R. Testylier, T. Dang, and A. Girard, *Reachability Analysis of Polynomial Systems Using Linear Programming Relaxations*. Berlin, Heidelberg: Springer Berlin Heidelberg, 2012, pp. 137–151.
- [17] T. Dang and R. Testylier, "Reachability analysis for polynomial dynamical systems using the bernstein expansion." *Reliable Computing*, vol. 17, no. 2, pp. 128–152, 2012.
- [18] D. Lee and K. Turitsyn, "Dynamic polytopic template approach to robust transient stability assessment," *arXiv preprint arXiv:1705.01189*, 2017.
- [19] D. Bertsimas and J. N. Tsitsiklis, *Introduction to linear optimization*. Athena Scientific Belmont, MA, 1997, vol. 6.
- [20] M. A. Duran and I. E. Grossmann, "An outer-approximation algorithm for a class of mixed-integer nonlinear programs," *Mathematical Programming*, vol. 36, no. 3, pp. 307–339, 1986.
- [21] W. Lohmiller and J.-J. E. Slotine, "On contraction analysis for non-linear systems," *Automatica*, vol. 34, no. 6, pp. 683 – 696, 1998.
- [22] H. D. Nguyen, T. L. Vu, J.-J. Slotine, and K. Turitsyn, "Contraction analysis of nonlinear dae systems," *arXiv preprint arXiv:1702.07421*, 2017.